Original Research Article

Application of SRTM DEM and Electrical Resistivity Techniques to Delineate Favourable Borehole Sites for Groundwater in Parts of Minna Sheet 164 SW, North-Central Nigeria

ABSTRACT

A combination of Shuttle Radar Topographic Mission (SRTM) Digital Elevation Model (DEM) and electrical resistivity were applied in parts of Minna, Sheet 164 SW, North-Central Nigeria to delineate favourable sites for drilling boreholes. Lineaments were extracted from derivative map of SRTM DEM datasets. Selected thematic layers which included lineaments, geologic structure and parametric maps derived from Vertical Electrical Sounding (VES) data were integrated and modelled using ArcGIS to generate a groundwater potential map of the area. Seventy VES were conducted using the Schlumberger array with a maximum AB/2 distance of 100 m and 500 m spacing between each VES sounding stations, to study the variation of resistivity of the ground at variable depths. Geologic mapping results revealed granite as the major lithology with schist occurring in the east. Principal joint directions and automated lineaments map of the combined four relief images trend in the NE - SW direction indicating weathering and probable high groundwater potentials along this direction. VES results revealed up to six geoelectric layers with different resistivities and depths. Six different geoelectric curves were generated from the analysis namely: HA, AA, HK, AK, KH and QH portraying various aquifers within the region. VES results also revealed that the area has undergone slight weathering (less than 6 metres in most parts) and is fractured from place to place. The fractures were found to be convergent to the middle portion of the study area indicating more groundwater accumulation towards that direction. Drill depths in this area should target a minimum of 100 m to ensure sufficient and sustainable supplies to drilled wells.

Keywords: SRTM DEM, Vertical Electrical Sounding (VES), Electrical Resistivity, Groundwater, Lineament

1. INTRODUCTION

Water is a precious and exceptionally important natural resource, without which life is not possible. Water is utilized daily for domestic, commercial, agricultural, industrial and recreational purposes. Civilizations have flourished with the development of reliable water supplies and have collapsed as water supplies failed (Fetter, 2012). In areas underlain by unconsolidated sediments, groundwater is often easy to find because it is present almost everywhere. However, in crystalline basement and consolidated sedimentary terrains, groundwater may only be present in useful quantities within fractured or weathered (Yaya, 2012). These facts dictate the use of a variety of information sources and techniques.

Groundwater exploration and development for rural, urban and industrial supplies presently takes many forms. Much emphasis has been placed recently on geophysical surveys alone, chiefly the electrical resistivity method (Idris, 2000). Minna, like most urban cities in Nigeria lack adequate supply of potable water for years now, wells and boreholes have cushioned the effect of the grossly erratic municipal water supply in the city. Most wells are seasonal, thriving best at rainy seasons; most boreholes too have taken the same trend providing low yield of water throughout the seasons.

Ten years ago, boreholes of thirty to forty metres thrived in Minna, but this is no longer the case; the aquifers at such depths have been overwhelmed by population growth and other environmental conditions. Further pressure is anticipated by the year 2020 considering the annual growth rate of 3.4 %. (NPC, 2006). Currently, the quest for water led to many geophysical survey recommendations which have yielded low productive wells within the city causing people to lose much money (Ejepu et al., 2017). The intensified usage of ‘‘water witching’’ for groundwater exploration which anchors its belief on the premise that groundwater can be accessed at further depths. This is not backed with sound scientific principles, thus, exacerbating the existing challenges. Hence, employing known and proven scientific method such as the combination of geology remote sensing and electrical resistivity methods will delineate potential zones in the study area so as to provide a framework for the development of groundwater resources in the area.

Integration of remote sensing and resistivity methods for groundwater exploration has been conducted by several authors (Akinluyi *et al.,* 2021; Omolaiye *et al.,* 2020; Mohamaden *et al.,* 2017). Their aim was to map and delineate regions of good groundwater prospects in a region. The basis for the research has also anchored on providing an environment suitable for economic extraction of groundwater resources. Other methods have been adopted to delineate groundwater potential zones using multi-parameter integration with different levels of successes. (Ejepu *et al.,* 2015; Abdullahi and Ejepu, 2018, Ejepu, 2020; Mirzaei *et al.,* 2020).

The basic challenge has been that interpretation of geophysical anomalies have not been accurately anchored on local hydrogeological constrains and factors. This has not helped in the reduction of the increasing failure rates recorded in borehole drilling and groundwater development activities (Ejepu *et al.,* 2017, Dan-Hassan, 2017)

The research therefore is aimed at delineating groundwater potential zones in the study area based on the integration of SRTM DEM, geological and electrical resistivity datasets. The objectives of the study are to delineate structures / lineaments from the SRTM DEM and carry out geologic field mapping of the study area on a scale of 1:25,000. Verification of these lineaments was done by acquisition, analysis and interpretation of VES data. Integration of these datasets led to the delineation of areas/zones of varying groundwater potentials.

1.1 Study area

Minna, the capital of Niger state is located within the north central part of Nigeria. The study area is in a part of Minna town between latitudes N9º35'24" to N9º38'24"; and longitudes E6º31'12" to E6º34'12", on a topographic map 1: 50,000 extending to parts of Bosso and Chanchaga Local Government Areas of Niger State. The total area coverage is approximately 30.69 km^2 (5.54 km by 5.54 km). The study area is accessible through a major road that cuts through the city centre connecting the city gates, the western and eastern bye-pass, minor roads that connect areas within the city, and footpaths connecting houses. The Lagos – Kaduna rail line also passes through the city. The location map of the study area is shown in Figure 1.

The relief in most part of the study area is plain land that has gentle slopes except towards the north-eastern parts opposite the College of Health Technology, Maitumbi area, along David Mark road, and parts of Tunga where the elevation is high. The elevations above sea level range from 207 m to 306 m. The drainage pattern is dendritic and the rivers derive their water from the Bosso dam and draining finally into river Chanchaga. Concrete drainages have replaced most of the river channels to curb flooding within the city.

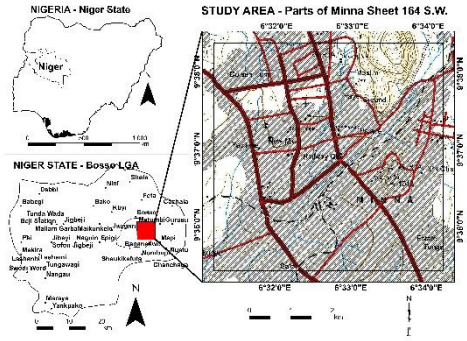

Figure 1: Location map of the study area.

1.2 Climate and vegetation

The study area is characterized by two distinct seasons; the rainy and dry seasons. The rainy season starts from April to October with its peak in August, while the dry season from November to March with its peak in the months of February and March having very high temperatures. The two seasons are often marked by a somewhat transitional period in April and November. The months of November to January are characterized by the harmattan which is the cold and dry weather conditions under the influence of the northeast trade winds. The annual mean temperature ranges from 27°C to 35°C with estimated yearly rainfall of 2500mm and average humidity of 27% (NIMET SRP, 2020)

The vegetation is Guinea Savannah characterized by grasses and short trees which are interspersed with stunted shrubs, the major species of trees being shea butter and locus bean trees; however, the area mapped is devoid of much vegetation because of urbanization (Ejepu and Olasehinde, 2014).

2. METHODOLOGY

2.1 Geological mapping

Geological mapping of the study area was done by both traverse and exposure mapping techniques on a scale of 1: 25,000. A total area of 30.69 km^2 (5.54 km x 5.54 km) was covered and forty-eight (48) rock exposures were studied during the exercise. The mapping involved observation, description and collection of data and rock samples from outcrops. Rocks were carefully observed using both the naked eyes and hand lens. Measurements of the orientation of geological planes and the angle of dip were made and recorded.

2.2 Lineament Data Extraction from SRTM DEM

The SRTM DEM was used to create shaded relief maps. The application of different sun azimuth values and elevation angles to the shaded relief was performed in order to extract manually digitised lineaments observed in various orientations. The value used for sun elevation angle was 25°, while for azimuths 0°, 45°, 90°, 135°, 180, 225°, 270°, 315°. The combinations of the eight shaded relief images were computed by using the GIS overlay technique, where the first four shaded relief images were overlaid to produce one image with illumination directions of 0°, 45°,90° and 135°. The second overlay is to produce one image with illumination directions of 180°, 225°, 270° and 315°. Finally, the combined image was used for automatic lineaments extraction over the study area. These methods were adapted from Sander, 1996; Sener *et al.,* 2005 and Rahiman and Pettinga, 2008. The lineament extraction algorithm of PCI Geomatica software (Geomatica, 2015) was used and it consist of edge detection, thresholding and curve extraction (Abdullah *et al.,* 2010; Aliko and Igwe, 2018). These steps were carried out over the two shaded relief images under the default parameters of the software (Table 1).

Table 1: Parameters used to extract lineaments from SRTM DEM using Geomatica software

NAME	DESCRIPTION	VALUES
RADI	Radius of filter in pixels	12
GTHR	Threshold for edge gradient	90
LTHR	Threshold for curve length	30
FTHR	Threshold for line fitting error	10
ATHR	Threshold for angular difference	30
DTHR	Threshold for linking distance	20

2.3 Lineament Analysis

The statistical analyses of the lineaments in the present study were based on the length and total number of the lineaments. The maximum, minimum and average length as well as the standard deviation of the length of the lineaments were also analysed. Rose diagram analyses were generated to show the orientation distribution of the lineaments. Rockworks 16 (RockWare Inc., 2018) software tools were utilized to construct rose diagrams.

2.4 Field Investigations (Ground Truthing)

Field investigation was done so that accurate correlations may be made with structural data obtained in the field and lineaments delineated from the SRTM DEM data. Priority was given to those areas that have prominent anomalies, contact locations and lineament coincident regions.

2.5 Vertical Electrical Sounding (VES)

The equipment used for the resistivity field measurements was a Geotron resistivity meter. Measurements were taken with the cycle selector switched for four averaged readings. Though, there are many electrode arrays that could be used in resistivity survey; Wenner, Schlumberger, pole - dipole and double dipole arrays, the Schlumberger electrode configuration was employed for the VES conducted in the project area because field operation is easier and signal- noise ratio is minimal. The maximum current electrode separation (AB) was 200 m. The potential electrodes were expanded symmetrically about a fixed centre of spread (Parasnis, 1986, Kearey & Brooks, 1991). A total of seventy (70) VES stations spread in seven (7) profiles were established (Figure 2).

The resistivity data were interpreted both qualitatively and quantitatively using computer based interpretative modelling. The field results were improved upon by employing an interactive (iterative) computer programme. Finally, the interpretation of the geoelectric parameters (resistivity and thickness) in terms of subsurface geology and groundwater conditions of the study area.

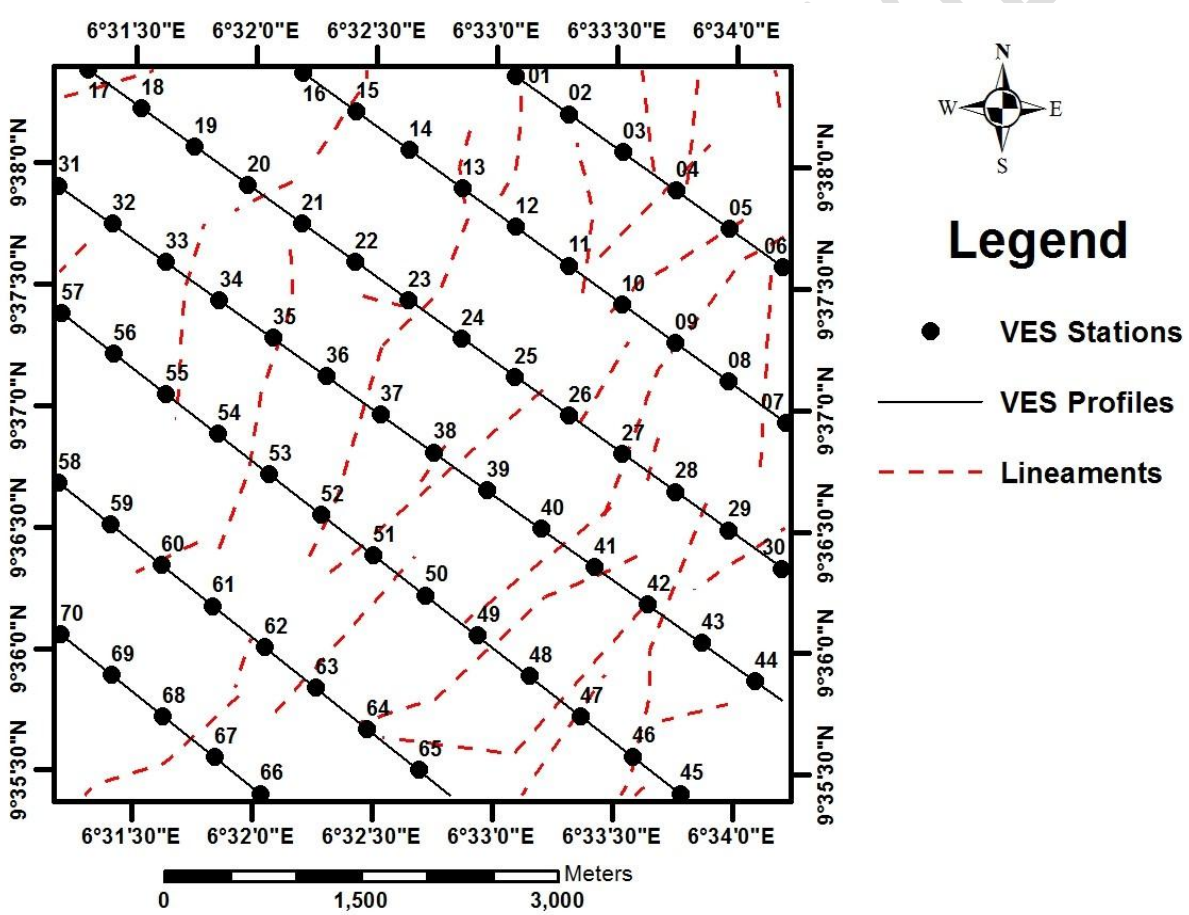

Figure 2: VES sounding stations along 7 Profiles (Profiles 1 to 7 from top to bottom). The spacing between VES sounding stations are 500 m apart.

The program used in the interpretation of the VES data is IPI2WIN version 3.01 (Bobachev, 2002). Consequently, the interpreted geo-electric parameters were used to plot the pseudo cross-sections and the resistivity sections of the VES profiles.

The reduced and filtered VES data along all seven survey profiles were used to construct the pseudo cross-sections so as to identify the distribution of different resistivity values in the lateral and vertical direction. The pseudo cross-sections of the VES data along all profiles are constructed using the IPI2WIN software. The qualitative interpretation of pseudo-section gives preliminary idea for the presence or absence of groundwater potential at a given area. The final result from one dimensional inversion of VES data along all survey lines were used to construct the resistivity cross sections in order to identify the distribution of different lithologic units in the vertical direction.

3. RESULTS AND DISCUSSION

3.1 Lineament extraction from SRTM DEM

The results from the automatic extraction of lineaments from composite shaded relief SRTM DEM (Figure 3a and 3b) and hence, indicate that the trend of the lineaments are dominant in the NE –SW direction (Figure 4a and 4b). In addition, these particular lineaments/faults seem to correspond to stream segments (Figure 4a and 4b). This direction is parallel to the regional fracture orientation of the area. The NE-SW lineaments (Figure 5a and 5b). imply the current tectonic regime of the area (Oluyide, 1988; Olasehinde, 1999; Olasehinde *et al.,* 2013). These lineaments informed the positioning of the profile orientations for the VES sounding. This was oriented orthogonal to these directions.

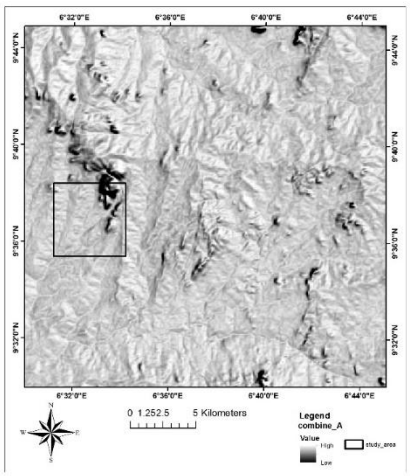

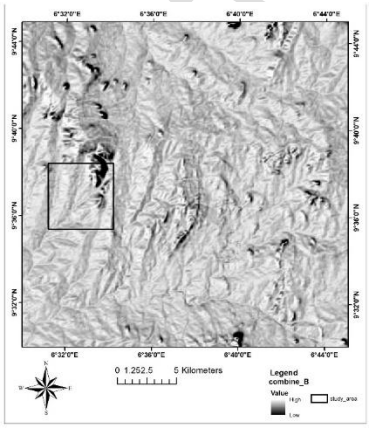

Figure 3(a) **Figure 3(b)**

Figure 3(a): Combined shaded relief images with sun angle of 0°, 45°,90° and 135°

Figure 3(b): Combined shaded relief images with sun angle of 180°, 225°, 270° and 315°

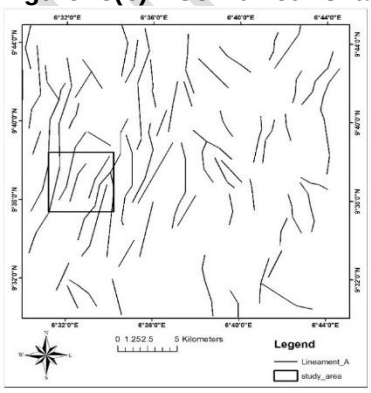

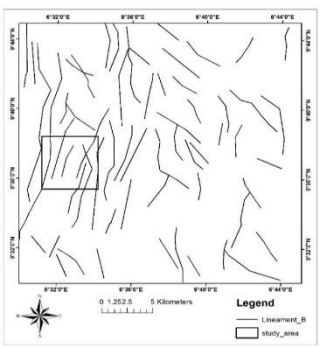

Figure 4a **Figure 4b**

Figure 4a: automatic lineament map of combined shaded relief images with sun angle of 0°, 45°, 90° and 135°.

Figure 4b: automatic lineament map of combined shaded relief images with sun angle of 180°, 225°, 270° and 315°

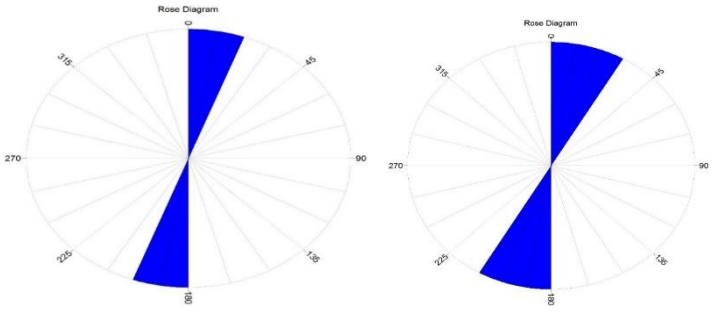

Figure 5a **Figure 5b**

Figure: 5a: Rose diagram of automatic lineament map of combining four shaded relief images with sun angle of 0°, 45°, 90° and 135°

Figure 5b: Rose diagram of automatic lineament map of combining four shaded relief images with sun angle of 180°, 225°, 270° and 315°

3.2 Geology of the study area

3.2.1 Lithological units

Information collected during field mapping of rock samples reveal that the study area falls within the Basement Complex and is underlain predominantly by granite showing low lying massive exposures (Rahaman, 1988). These rocks are slightly weathered with an observed weathering profile of less than six metres in most part. The black spots on the rock are biotite, the smaller smoky grains are quartz and the white grains are plagioclase feldspars.

The eastern portion of area is underlain by an amphibole and schist. The schist covers less than ten percent of the study area and are exposed as flat ridges which are levelled and highly weathered. They are greenish in colour when viewed in hand specimen, with fine to medium texture,

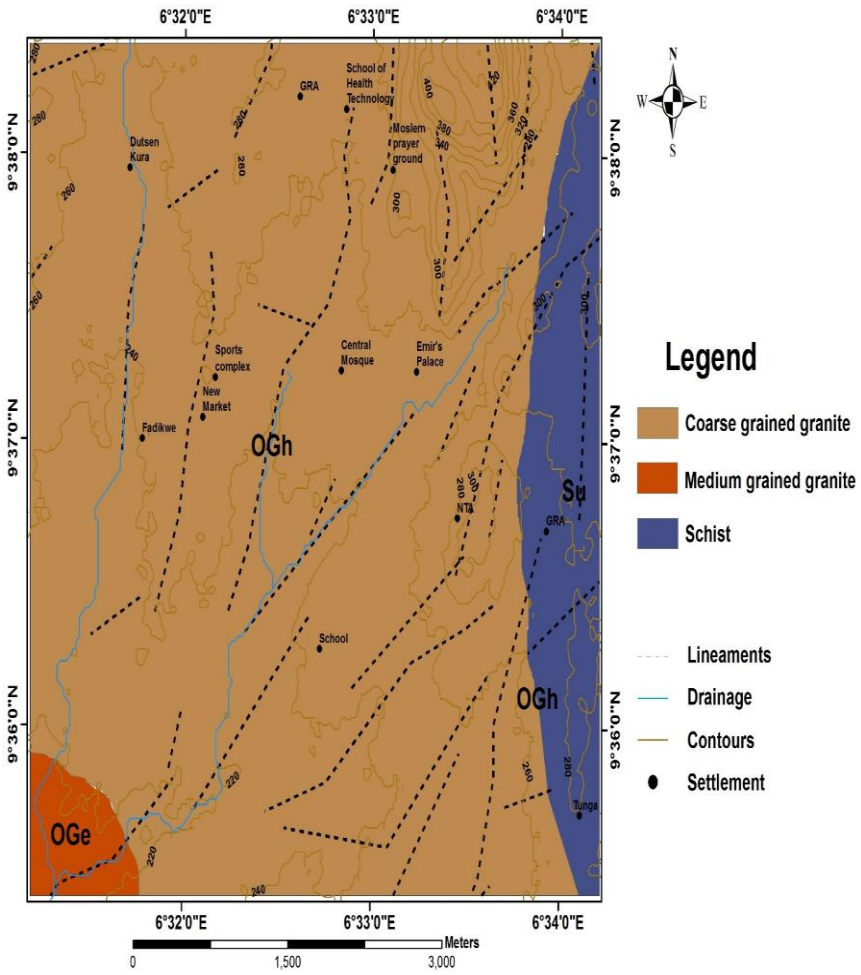

Figure 6: Geologic Map of the Study Area

3.2.2 Structural geology

The common structures found in the study area were mostly fractures (fissures, cracks or joints). A weathered granitic rock riddled with a system of joints was found within the study area. The Rosette diagram obtained from joint readings on rocks of the area (Figure 7) reveals that the principal joints trends in the NNE - SSW direction while the minor joints trends in the W – E direction.

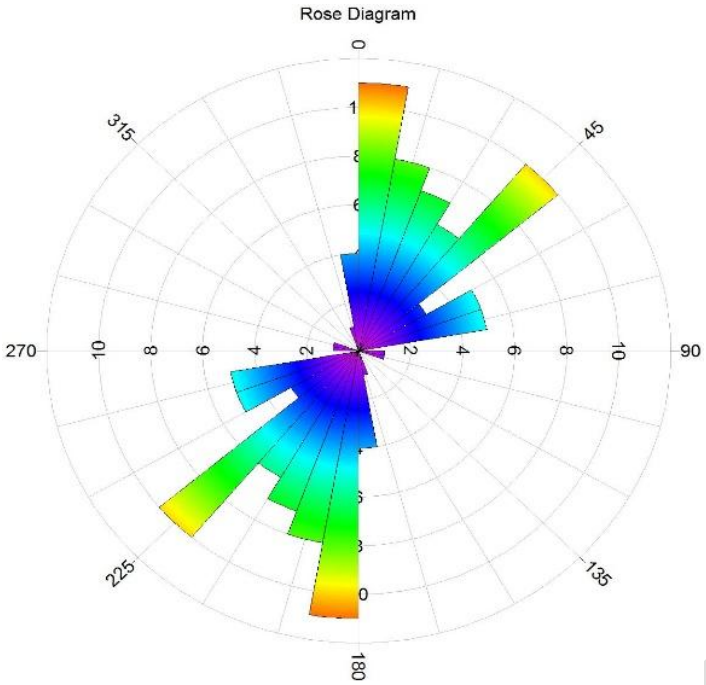

Figure 7: Rosette diagram of joint directions.

3.3 Discussions and Interpretation of VES

3.3.1 Interpreted VES Curves

An illustration is made using six interpreted VES curves, one each from the curve types and these are given in Figure 8. In the six sounding curve types, a 3 to 5 layer of the subsurface is represented (with the AB/2 of 100 m used for the survey) namely: HA, HK, AA, KH, QH and AK portraying various potential aquifers within the region. The HA-type covers 45%; the HK-type covers 26%; the AA-type covers 11%; the AK-type covers 9% while the remaining 9% of the total surveyed points is covered by the KH and QH-types. The areas marked by HA-type have fractured zone existing directly below the weathered zone (McFarlane, 1989), the groundwater yield in these areas could not be high because the density of the fractured columns is not high (Olorunfemi, 2009).

The areas marked by HK type, have the fractured zones concealed beneath the fresh basement, such areas may not have any hydraulic connectivity between the weathered and fractured zones but complements each other if wells are sunk into them, the curve type generally produce prolific wells especially where the weathered and fractured layers are thick. The areas marked by KH type are characterised by thin top soil/ weathered zones and the fractured zones are confined within the fresh basement as such, these areas may have significant yield of water only when the fracture density is high and the fractured column is thick. The areas marked by QH and AA types have sharp transition between the weathered and the fresh basement, the weathered layer is the sole aquifer unit and groundwater yield here is determined by the degree of shaleliness of the weathered layer, low yield is obtained if underlain by schist or clay (Olugboye, 2008).

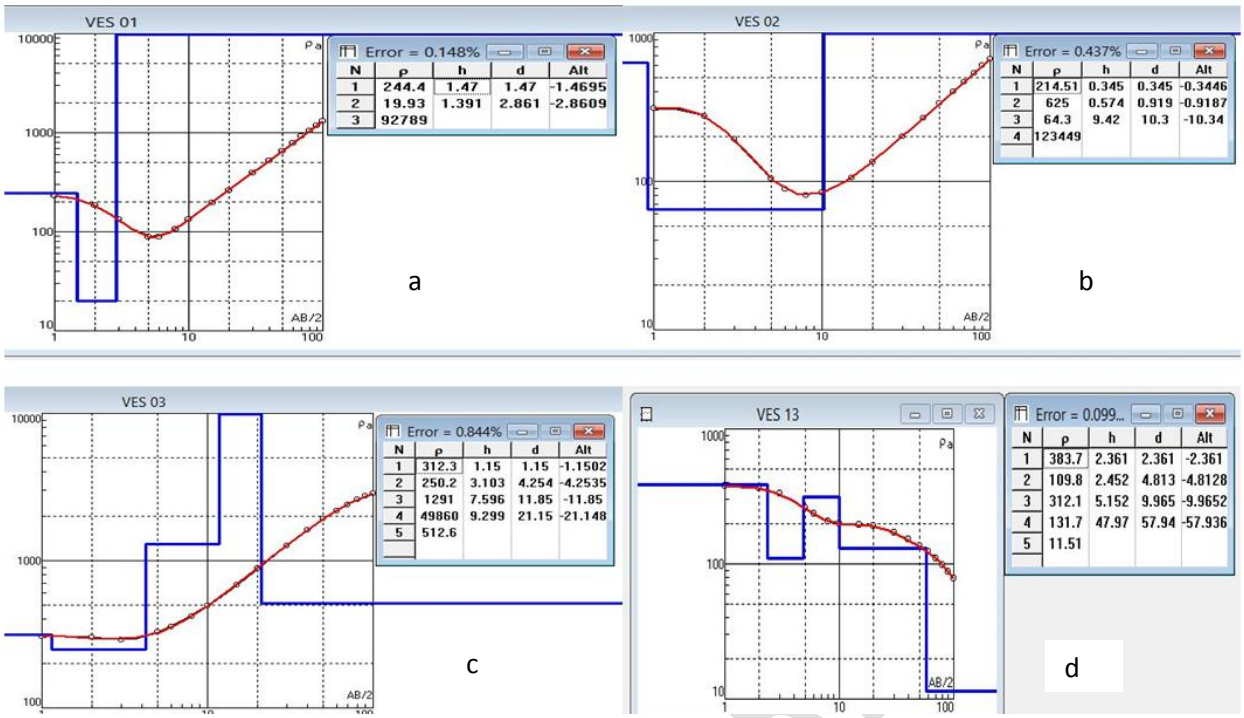

Figure 8: Typical (a) H-Type curve, (b) HA – Type curve (c) and (d) other 5 – layer curve types.

3.3.2 Pseudo cross-section and Resistivity cross-section of the Profiles

Profile 1 trends SW to NE through Soundings VES01 through VES06.It has a length of almost 2500m and is oriented orthogonally to the delineated lineaments. Figure 9 shows the resulting pseudo- and resistivity cross-section of Profile 1 and it generally shows a low homogeneous resistivity all across the pseudo cross-section in the uppermost layers. The values of the geoelectric layers were modelled having a top to bottom layer with varying resistivity values ranging from 15 to 28000Ωm. Top and second layer thicknesses are generally thin in all the sounding stations. The anomalously very low resistivity structure is found between VES05 and VES06.

Profile 2 runs a total length of 4500 m north-west to east coveringVES07 to VES16. The pseudo and resistivity cross-section of this profile is presented in Figure 10. Here the pseudo cross-section resistivity range between 89 - 710Ωm. A second layer of low resistivity is consistent with VES stations located in the study area are thicker at VES10 and VES15. The pseudo cross-section has an anomalously low resistivity structure in VES08 and VES07. At VES12, an anomalously high resistivity could be observed at VES12. This could be as a result of an almost outcropping rock that has not been weathered. The resistivity distribution for this pseudo cross-section is higher on the left-hand side of the profile, while the right-hand side of the profile is considerably smaller.

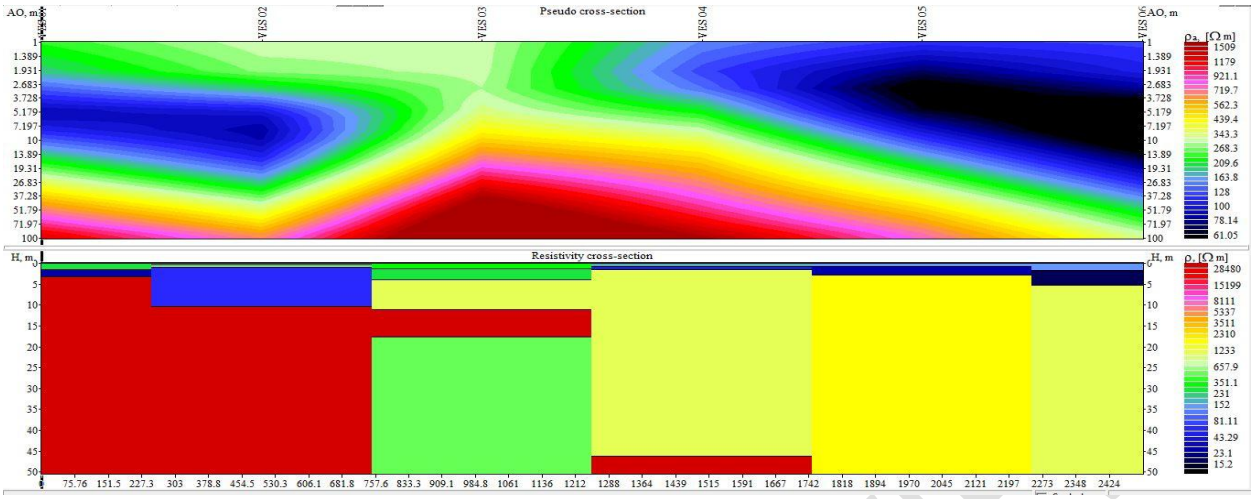

Figure 9: Pseudo cross-section and Resistivity cross-section of Profile 1 in the study area.

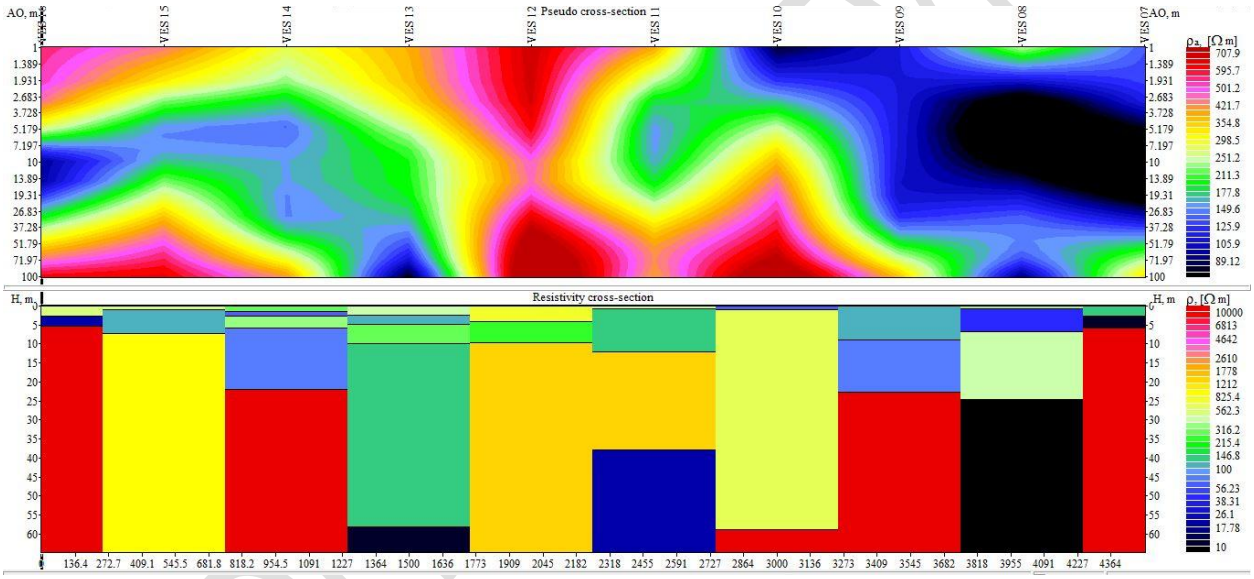

Figure 10: Pseudo cross-section and Resistivity cross-section of Profile 2 in the study area.

The varying degrees of resistivity values in the pseudo cross-section in profile 3 (Figure 11) are due to the amount of saturation and clay content present within this unit. The additional layer of high resistivity beneath this VES could be caused by the presence of dry large gravel with little sand and clay. This top layer has thickness generally below 5 m The second layer has low resistivity of range 20 - 400 Ωm, observed all throughout the resistivity cross-section. The region with anomalously very low resistivity occupies VES18 to VES21 with resistivity values ranging from 10 to 50 Ωm.

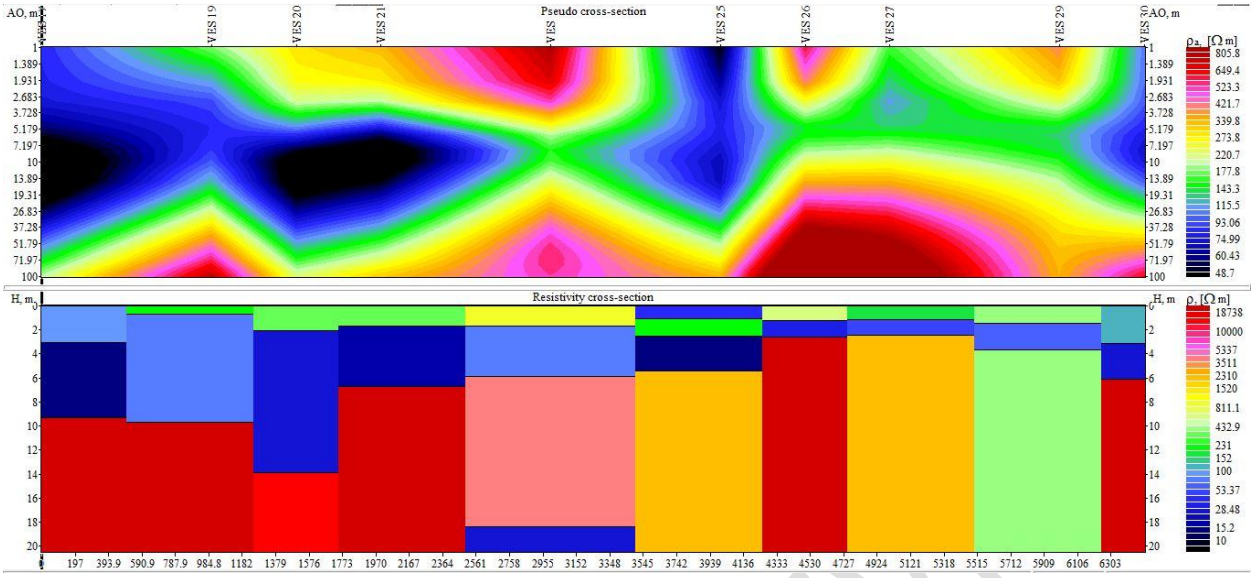

Figure 11: Pseudo cross-section and Resistivity cross-section of Profile 3 in the study area.

Profile 4 is the longest in all the profiles. It trends NW to SE through Soundings VES31 through VES44. It has a length of almost 6700 m and is oriented orthogonally to the delineated lineaments. Figure 12 shows the resulting pseudo- and resistivity cross-section of Profile 4 and it generally shows low homogeneous resistivity structures around the central portions of the pseudo cross-section. Very high values of the geoelectric layers were modelled around VES34 to VES37 and VES41. It has a top to bottom layer with varying resistivity values ranging from 10 to 28000 Ωm. Top layer thicknesses are generally thin but second layer thicknesses are generally moderate in all the sounding stations.

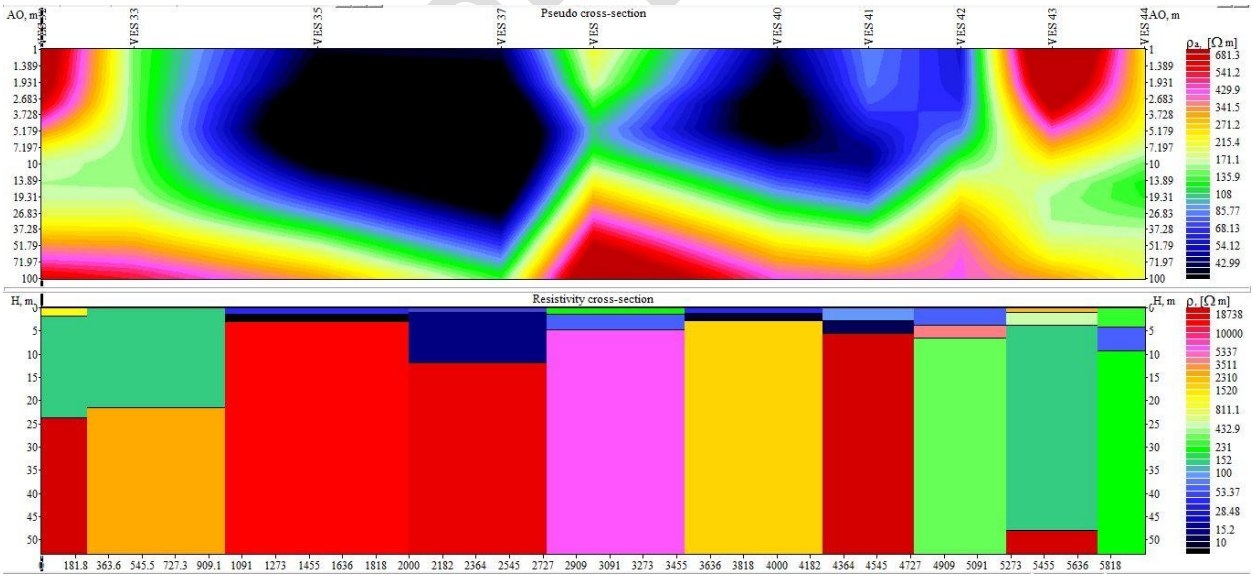

Figure 12: Pseudo cross-section and Resistivity cross-section of Profile 4 in the study area.

Profile 5 (Figure 13) which covers VES45 to VES57 shows thin soil and weathered layers with slight fractures inferred at the flanks of the pseudo cross-section. This imply that areas around these points will have relatively higher groundwater potential; places that have undergone appreciable weathering but not

fractured may mean that the weathered portion is expected to accumulate water most especially as the soil layer is also relatively thick.

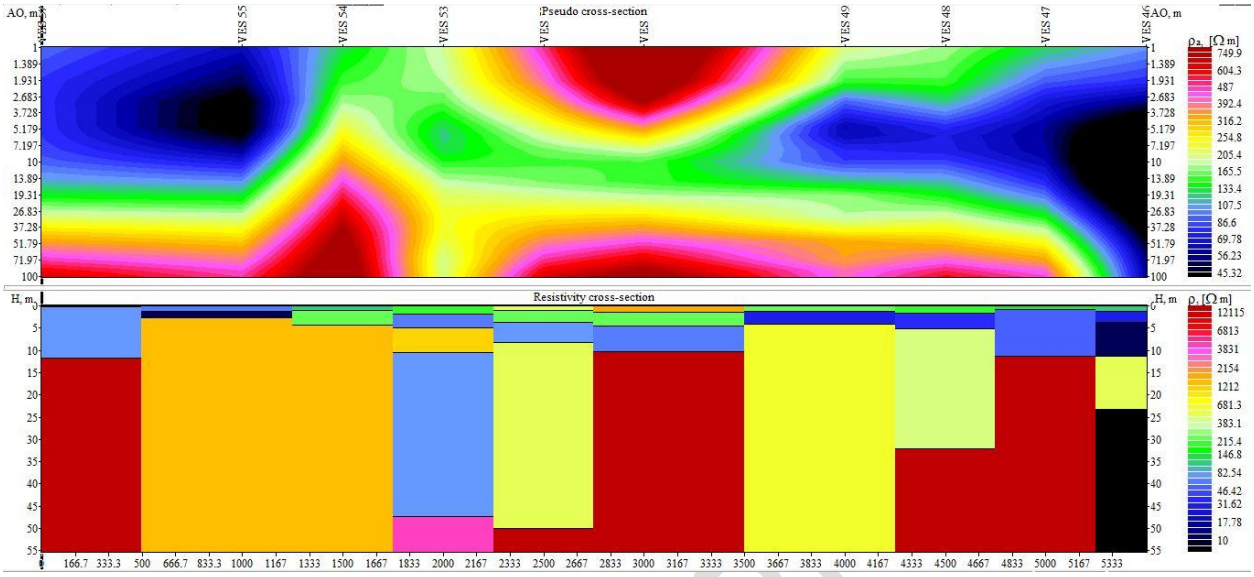

Figure 13: Pseudo cross-section and Resistivity cross-section of Profile 5 in the study area.

Profile 6 trends SW through Soundings VES58 through VES65. It has a length of almost 3800 m and is oriented orthogonally to the delineated lineaments. Figure 14 shows the resulting pseudo- and resistivity cross-section of Profile 6 and it shows a low homogeneous resistivity at the right hand side of the pseudo cross-section in the uppermost layers. The values of the geoelectric layers were modelled having a top to bottom layer with varying resistivity values ranging from 7 to 31000 Ωm. Top and second layer thicknesses are generally thin in all the sounding stations. The anomalously very low resistivity structure is found between VES59 and VES61.

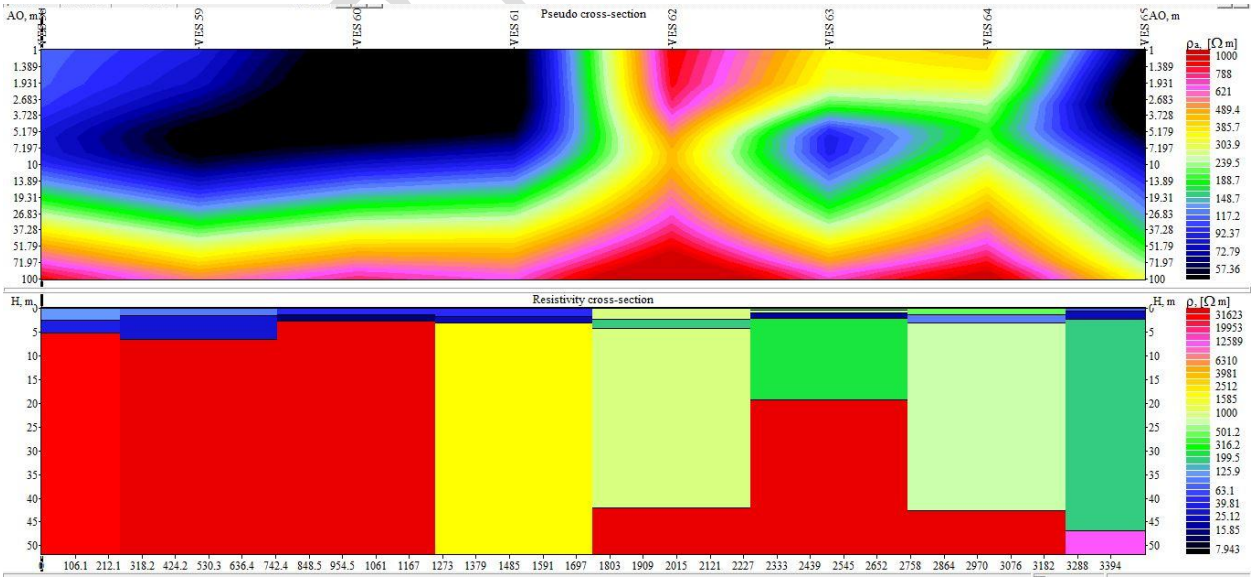

Figure 14: Pseudo cross-section and Resistivity cross-section of Profile 6 in the study area.

Profile 7 (Figure 15) runs a total length of 2 km in the SW quadrant of the mapped area covering VES66 to VES70. The pseudo and resistivity cross-section of this profile is presented in Figure 4.27. Here the pseudo cross-section resistivity range between 28 - 900 Ωm. A second layer of low resistivity is consistent with VES stations located in the study area are thicker at the various sounding stations compared to other sounding stations un the study area. The pseudo cross-section has an anomalously very low resistivity structure across the profile.

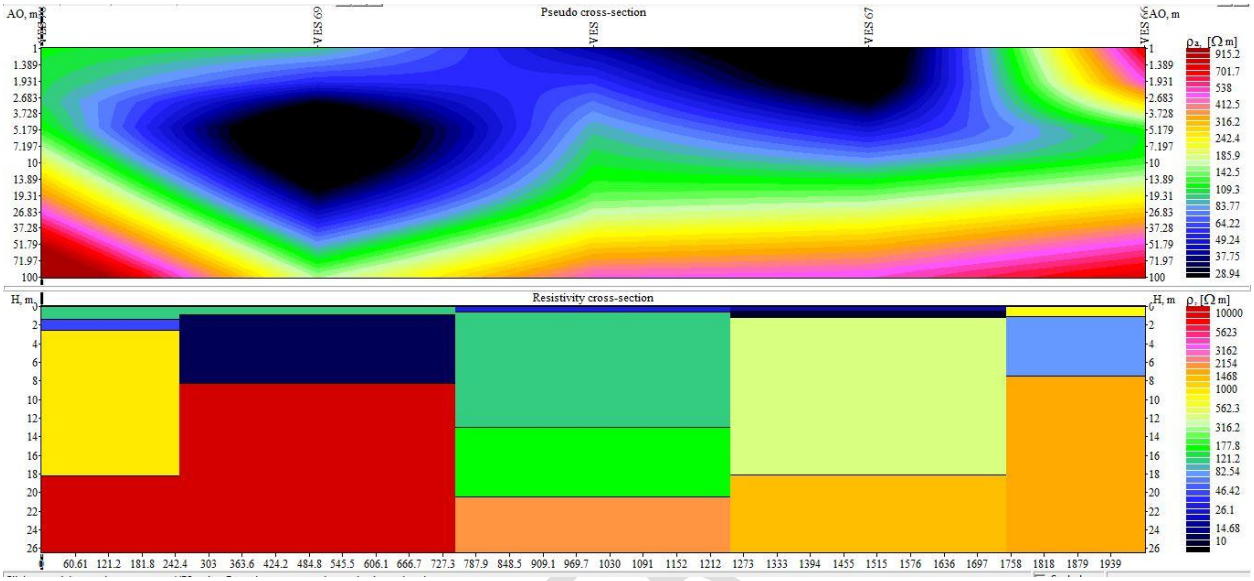

Figure 15: Pseudo cross-section and Resistivity cross-section of Profile 7 in the study area.

The implications of these results indicate that areas with thin top soil and thick weathered layer with evidence of fracturing has better groundwater prospect than areas without fracturing. Hence, a combination of thickly weathered residuum and evidence of fracturing at depth gives an indication of good groundwater potential at any point.

3.3.3 Depth to Basement

The study area has undergone slight weathering, varying from place to place with the major portions having a weathering thickness of less than six metres and apparent resistivity values less than 150 Ωm. The thicker the weathering profile of the basement, the more water it accumulates as such, areas with weathered thicknesses above six metres will have more weathered aquifer potential. Figures 16 shows the depth to basement which is very vital in groundwater potential determination, the thicker they are, the more they accumulate groundwater and the higher the potential of such areas.

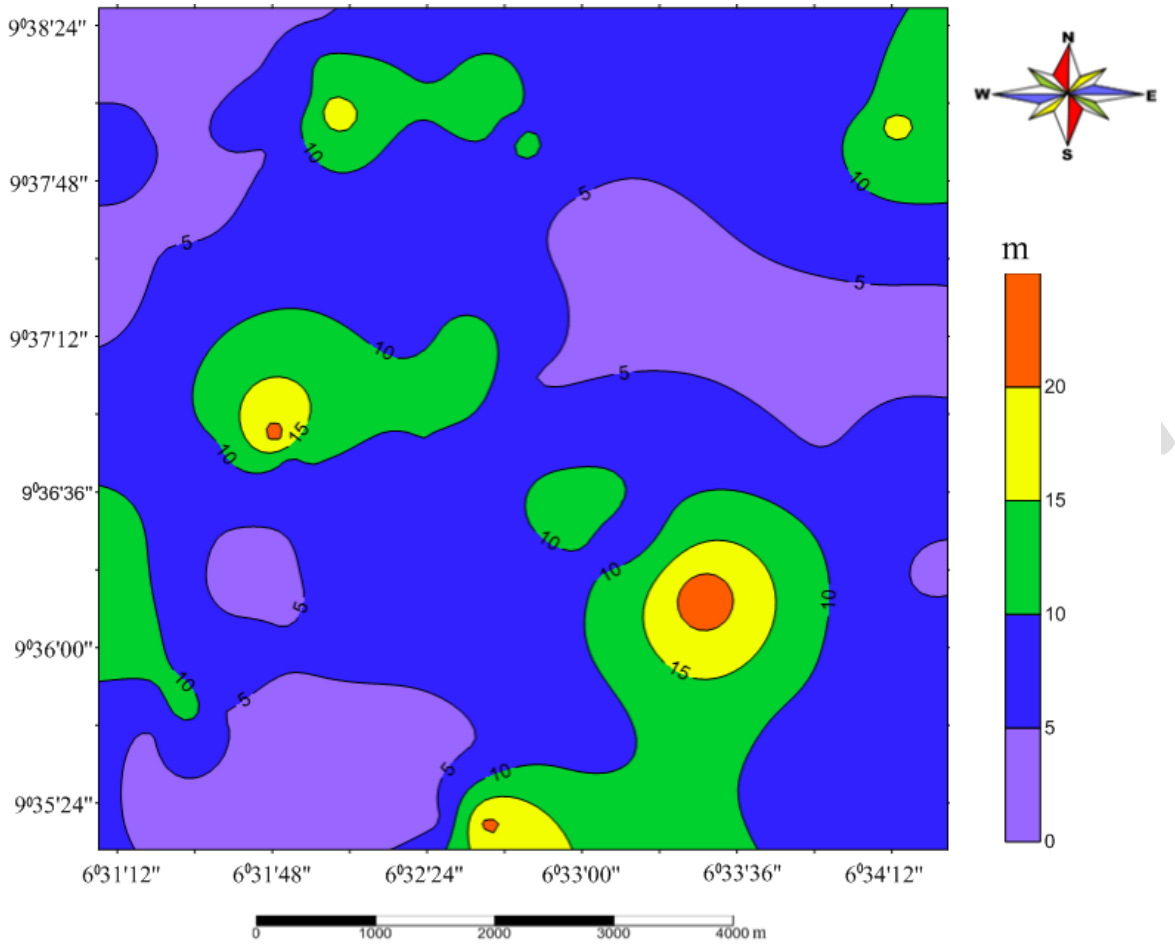

Figure 16: Depth to basement in the study area

Figure 17 shows the groundwater potential map of the study area deduced from superimposing combination of results from the geology and interpretations made from electrical resistivity data. Areas that are coloured green have high groundwater potential; those coloured blue have medium groundwater potential while those coloured red have low groundwater potential. This map revealed that the fracture density has a strong effect on groundwater availability. This is so because fracture density is higher at the middle portion of the study area. Nevertheless, for more detailed groundwater development campaign, it is still necessary to conduct more detailed fracture mapping and geophysical surveys.

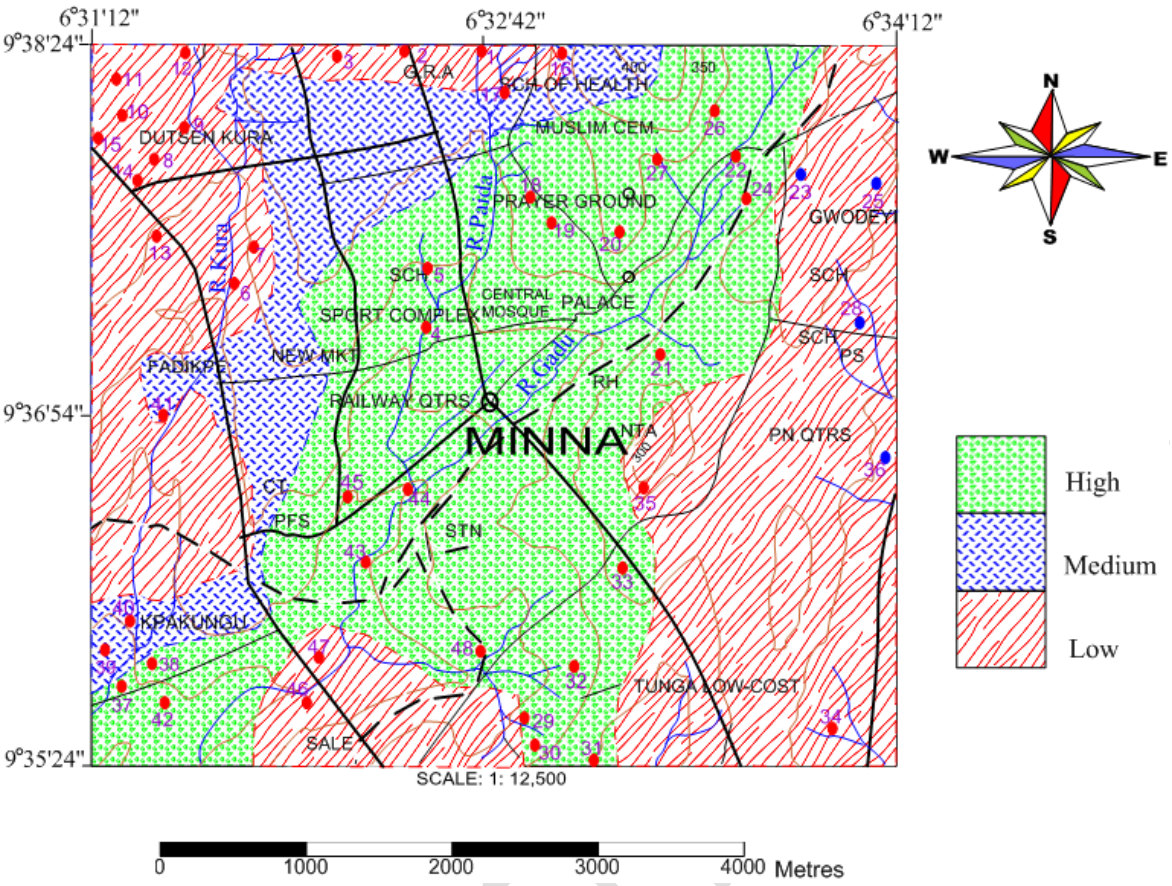

Figure 17: Groundwater potential of the study area

4. CONCLUSIONS

Geologic mapping revealed that the study area is underlain predominantly by granite while the eastern area is underlain by rocks belonging to the metasedimentary rocks – amphibolite complex made up of schists. The measurements obtained from joint directions reveals the principal joints trending in the NNE - SSW direction and the minor joints in the W – E directions indicating weaknesses in those directions and thus high potential in that direction.

SRTM DEM have been successfully employed to delineate and map lineaments in the study area. The SRTM DEM images pronouncedly revealed regional lineaments associated with drainage channels and other geomorphological features.

Vertical Electrical Sounding (VES) carried out in the study area were used to plot resistivity graphs, pseudo cross-sections, resistivity cross-sections and contour plots of depth to basement. The outcome showed topsoil thickness of less than four metres and weathering depths of less than six metres in most places (these supports wells) and an increasing groundwater potential towards the middle portion from the western and eastern parts of the study area. these results were used to categorise the study area into high, medium and low groundwater potential zones.

4.1 Recommendations

The yield of shallow boreholes in the area is dropping with increased demand for groundwater as a result of population increase. This intense abstraction has also caused the downward movement of water levels. Therefore, motorized boreholes should be drilled in the study area to at least 120 m and above for high and medium groundwater potential areas respectively to provide the area with lasting water solution. Boreholes sunk in medium potential areas could experience intermittent cutting and recharging if not deep enough. Hence, it is recommended that controlled groundwater abstraction method be used in medium groundwater potential areas.

REFERENCES

Abdullah, A., Akhir, J. M., & Abdullah, I. (2010). Automatic mapping of lineaments using shaded relief images derived from digital elevation model (DEMs) in the Maran–Sungi Lembing area, Malaysia. *Electronic Journal of Geotechnical Engineering*, *15*(6), 949-958.

Abdullahi, D.S., & Ejepu, J.S. Aeromagnetic and Resistivity Surveying for Delineating Optimal Sites for Groundwater development in part of Minna, Sheet 164 SW, North-Central Nigeria.

Ajayi, O., Abegunrin, O.O. (1994). Borehole failures in crystalline rocks of South-Western Nigeria. *GeoJournal* **34,** 397–405. https://doi.org/10.1007/BF00813135.

Akinluyi, F.O., Olorunfemi, M.O. and Bayowa, O.G. (2021). Application of remote sensing, GIS and geophysical techniques for groundwater potential development in the crystalline basement complex of Ondo State, South-western Nigeria. Sustainable Water Resources Management. Issue 1/2021.

Aluko, O.E., & Igwe, O. (2018). Automated Geological lineaments mapping for groundwater exploration in the basement complex terrain of Akoko-Edo area, Edo-State Nigeria using remote sensing techniques. *Modeling Earth Systems and Environment*, *4*(4), 1527-1536.

Bobachev, C. (2002). IPI2Win: A Windows Software for an Automatic Interpretation of Resistivity Sounding Data. PhD Thesis, Moscow State University, Russia, 2002.

Dan-Hassan, Mohammed. (2017). Review of Borehole Failures: Causes and Remedies. 10.13140/RG.2.2.13702.93768.

Ejepu, J.S. (2020). Regional Assessment of Groundwater Potential Zone Using Remote Sensing, GIS and Multi Criteria Decision Analysis Techniques. *NIGERIAN ANNALS OF PURE AND APPLIED SCIENCES*, *3*(3b), 99–111. https://doi.org/10.46912/napas.201.

Ejepu, J.S. and Olasehinde, P.I. (2014). Groundwater Potential Evaluation in the Crystalline Basement of Gidan Kwano Campus, Federal University of Technology, Minna, North-Central Nigeria Using Geoelectric Methods. Universal Journal of Geoscience 2(4): 123-132. http://www.hrpub.org. DOI: 10.13189/ ujg.2014.020403.

Ejepu, J.S., Olasehinde, P.I., Omar, D.M, Abdullahi, D.S., Adebowale, T.A., and Ochimana, A. (2015). Integration of geology, remote sensing and geographic information system in assessing groundwater potential of Paiko sheet 185 North-Central Nigeria. Journal of Information, Education, Science and Technology, Volume 2, Pages 145-155.

Ejepu, J.S., Olasehinde, P.I., Okhimamhe, A.A., and Okunlola, I. (2017). Investigation of Hydrogeological Structures of Paiko Region, North-Central Nigeria Using Integrated Geophysical and Remote Sensing Techniques. Geosciences 2017, 7, 122. https://doi.org/10.3390/geosciences7040122.

Fetter, C.W. (2012). *Applied Hydrogeology,* New York NY: Prentice Hall, Oxford University press.

Geomatica (2015). Automatic Lineament Extraction Algorithm. http://www.pcigeomatics.com/pressnews/2015_PCI_Geomatica-15

Idris, N. A. (2000). A geophysical survey method for groundwater in crystalline rock terrain. Unpublished M. Tech Thesis, F.U.T. Minna.

Keary, P. and Brooks, M. (1991) An Introduction to Geophysical Exploration. 2nd Edition, Blackwell Scientific Publications, Oxford, 254 p.

McFarlane, M. J. (1989). A review of the development of tropical weathering profiles with particular reference to leaching history and with examples from Malawi and Zimbabwe. In: groundwater exploration and development in crystalline basement aquifers. Proceedings Zimbabwe, June 1987, vol. II, sessions 6-15, Commonwealth Science Council, Pall Mall, London, 95-145.

Mirzaei, L., Hafizi, M., Riahi, M. (2020). Exploration of Karst Groundwater using Electrical Resistivity Tomography and Remote Sensing, North East Khuzestan. *Journal of the Earth and Space Physics*, 46(2), 247-264. doi: 10.22059/jesphys.2020.295094.1007184.

Mohamaden, M.I.I., El-Sayed, H.M. and Mansour, S.A. (2017). Combined application of electrical resistivity and GIS for groundwater exploration and subsurface mapping at northeast Qattara Depression, Western Desert, Egypt, Egyptian Journal of Basic and Applied Sciences, Volume 4, Issue 1, Pages 80-88, ISSN 2314-808X, https://doi.org/10.1016/j.ejbas.2016.10.003. (https://www.sciencedirect.com/science/article/pii/S2314808X16301464).

National Population Commission (NPC) (2006). Population and Housing Census Priority Tables, 2006. www.population.gov.ng.

Nigerian Meteorological Agency (NIMET). (2020). Seasonal Rainfall Prediction (SRP). https://www.nimet.gov.ng/category/nimet-2020-srp/

Olasehinde P. I. (1999): An integrated geologic and geophysical exploration technique for groundwater in the Basement Complex of West Central Nigeria. *Water Resources Journal*, 10, 46-49.

Olasehinde P. I., Ejepu S. J. & Alabi A. A. (2013). Fracture Detection in a Hard Rock Terrain Using Radial Geoelectric Sounding Techniques. Water Resources Journal 23(1&2), 1-19.

Olorunfemi, M.O. (2009). Groundwater exploration, borehole site selection and optimum drill depth in basement complex terrain. *Journal of water resources*, 2, 5 – 10.

Olugboye, M. O. (2008). *Hydrogeological Practices (with Application to Nigerian Groundwater Terrains)*. Ilorin. PIOS Publishers.

Oluyide, P.O. (1988). Structural trends in the Nigerian Basement Complex. In: Precambrian Geology of Nigeria. *Geological Survey of Nigeria*, pp. 93 - 98.

Omolaiye, G. O., Ilesanmi A., Adebowale R., Akinwale A, Akinpelumi O., and Kayode S. O. (2020). Integration of remote sensing, GIS and 2D resistivity methods in groundwater development. Applied Water Science. 10. 10.1007/s13201-020-01219-x.

Parasnis, D.S. (1986) Principles of Applied Geophysics. 4th Edition, Chapman and Hall, London, Vol. 360, 104-116.

Rahaman, M.A. (1988). Recent advances in the study of the Basement Complex of Nigeria. Precambrian Geology of Nigeria, *Geological Survey of Nigeria Publications,* 11-43.

Rahiman, T. & Pettinga, J., (2008). Analysis of lineaments and their relationship to Neogene fracturing, SE Viti Levu, Fiji: Geological Society of America Bulletin, 120(11-12), 1544-1555.

Regional Assessment of Groundwater Potential Zone Using Remote Sensing, GIS and Multi Criteria Decision Analysis Techniques

Rockworks 16. RockWare Inc. 2221 East St. #1 Golden, CO 80401 USA. https://www.rockware.com/product/rockworks/

Sander, P. (1996). Remote Sensing and GIS for Groundwater Assessment in Hard Rocks: Applications to Water Well Siting in Ghana and Botswana. PhD dissertation, Chalmers University of Technology, Sweden, Publication A 80

Sener E., Davraz A. & Ozcelik M. (2005). An integration of GIS and remote sensing in groundwater investigations: A case study in Burdur, Turkey. Hydrogeology Journal, 13 (5-6), 826-834. http://dx.doi.org/10.1007/s10040-004-0378-5.

Yaya, O.O. (2012). *Groundwater investigation techniques*. A course module by the Federal Ministry of Water Resources & JICA: Arisekol press.